



## Phantom reflexes: Muscle contractions at a frequency not physically present in the input stimuli

E. Manjarrez<sup>a,\*</sup>, P. Balenzuela<sup>b</sup>, J. García-Ojalvo<sup>b</sup>, E.E. Vásquez<sup>a</sup>,  
L. Martínez<sup>a</sup>, A. Flores<sup>a</sup>, C.R. Mirasso<sup>c</sup>

<sup>a</sup> Instituto de Fisiología, Benemérita Universidad Autónoma de Puebla, 14 Sur 6301, Col. San Manuel, A.P. 406, Puebla, Pue., CP 72570, Mexico

<sup>b</sup> Departament de Física i Enginyeria Nuclear, Universitat Politècnica de Catalunya, Colom 11, E-08222 Terrassa, Spain

<sup>c</sup> Departament de Física, Universitat de les Illes Balears, E-07122 Palma de Mallorca, Spain

Received 19 July 2006; accepted 4 October 2006

### Abstract

In the motor system, the periodic stimulation of one Ia-afferent input produces reflex muscle contractions at the input frequency. However, we observed that when two Ia monosynaptic reflex-afferent inputs are involved the periodic muscle contractions may occur at a frequency physically not present in the afferent inputs even when these inputs are sub-threshold. How can the muscles respond with such phantom reflex contractions at a frequency physically absent in the sub-threshold Ia-afferent input stimuli? Here we provide an explanation for this phenomenon in the cat spinal cord, that we termed “ghost motor response”. We recorded monosynaptic reflexes in the L7 ventral root, intracellular potentials in the motoneurons, and the associated muscular contractions elicited by stimulation of the lateral and medial gastrocnemius nerves. By stimulating with periodic pulses of sub-threshold intensities and distinct frequencies of 2 and 3 Hz the lateral and medial gastrocnemius nerves, respectively, we observed monosynaptic responses and phantom reflex muscle contractions occurring at the fundamental frequency (1 Hz), which was absent in the input stimuli. Thus we observed a reflex ghost motor response at a frequency not physically present in the inputs. We additionally studied the inharmonic case for sub-threshold stimuli and observed muscular contractions occurring at much lower frequencies, which were also conspicuously absent in the inputs. This is the first experimental evidence of a phantom reflex response in the nervous system. The observed behavior was modeled by numerical simulations of a pool of neurons subjected to two different input pulses.

© 2006 Elsevier Ireland Ltd. All rights reserved.

**Keywords:** Coincidence; Ghost resonance; Missing fundamental illusion; Monosynaptic reflex; Facilitation; Motoneurons

### 1. Introduction

A major goal in neurophysiology is to understand how the central nervous system integrates the sensory information. A basic mechanism of integration is the

summation of sub-threshold synaptic potentials in spinal motoneurons (Lloyd, 1946; Granit et al., 1966; Kuno and Miyahara, 1969). This mechanism explains why motoneurons achieve threshold in response to the coincident occurrence of excitatory potentials. Here we show a related and simple phenomenon, based on the summation of synaptic potentials occurring at different input frequencies on motoneurons. We would like to test the hypothesis that reflex muscle contractions may occur at a frequency physically absent in the monosynaptic Ia

\* Corresponding author. Tel.: +5222 22 295500x7326;  
fax: +5222 22 295500x7323.  
E-mail address: [emanjar@siu.buap.mx](mailto:emanjar@siu.buap.mx) (E. Manjarrez).

sensory inputs, thus generating a phantom reflex contraction, i.e., a “ghost motor response”. We consider that the phantom reflex of the muscles is a kind of phenomenon based on simple principles, but not for this reason is not important. Our study shows that when two Ia-afferent inputs are activated the classical monosynaptic reflexes could occur at a frequency physically absent in the Ia-afferent inputs.

The present study was motivated by the mathematical model of Balenzuela and Garcia-Ojalvo (2005) to explain the neural mechanism for the binaural pitch perception (see also Chialvo, 2003). These authors studied a neural architecture consisting of two neurons described by the Morris–Lecar model, driven by noise and by two periodic signals of different frequencies ( $f_1 = kf_0 + \Delta f$  and  $f_2 = (k + 1)f_0 + \Delta f$ , where  $k > 1$ ), whose outputs (plus noise) impinge synaptically on a third neuron that integrates the two upstream input signals. According to this model, a neuron that receives synaptic inputs from two other neurons firing with distinct frequencies ( $f_1$  and  $f_2$ ) responds at the (lower) fundamental frequency  $f_0$ , which is missing in the input. We provide an experimental and theoretical explanation of a similar phenomenon we termed “ghost motor response” in the simplest synaptic pathway of the central nervous system: the circuit of the monosynaptic reflex of the cat spinal cord.

This study could be important to further understand how in more complex systems the nervous system integrates sensory information at a frequency physically absent in the sensory inputs.

## 2. Materials and methods

### 2.1. Preparation

Experiments were carried out in eight adult cats (2.0–3.5 kg). For surgery, anaesthesia was induced and maintained with halothane (5%) delivered in a mixture of 30% oxygen and 70% nitrous oxide. Atropine (0.05 mg kg<sup>-1</sup>) and dexamethasone (2 mg kg<sup>-1</sup>) were given at the beginning of the surgery. Guidelines contained in National Institutes of Health *Guide for the Care and Use of Laboratory Animals* (85–23, revised in 1985) were strictly followed. Level of anaesthesia was verified throughout the surgery by monitoring arterial blood pressure and by testing for the lack of withdrawal reflexes and muscle tone. Radial vein was cannulated to administer fluids and blood pressure was monitored from the carotid artery. A bicarbonate and glucose (5%) solution was delivered intravenously through the experiment at a rate of 5 ml h<sup>-1</sup>. Dextran and saline solutions were given. Blood pressure was maintained between 80 and 120 mmHg.

Lateral gastrocnemius (LG) and medial gastrocnemius (MG) nerves were dissected. The lumbo-sacral and low thoracic spinal segments were exposed and the dura mater

was removed. After these surgical procedures, the animal was mounted in a stereotaxic apparatus using spinal and pelvic clamps (for further details see Manjarrez et al., 2003, 2005). In some experiments, the left and right ventral roots L5–S2 were dissected and sectioned. Pools were formed with the skin around the exposed tissues, filled with mineral oil (after placement of the electrodes) and maintained at a constant temperature (37 °C). A mechanical precollicular-postmammillary decerebration was performed with removal of both cortices and all tissue rostral to the transection. After decerebration the anaesthetic was discontinued. Some animals were paralysed with pancuronium bromide (Pavulon, Organon), and artificially ventilated. At the end of the experiment each animal was euthanized with an overdose of pentobarbital.

### 2.2. Stimulation

LG and MG nerves were stimulated with sub-threshold single rectangular pulses of 0.1 ms. Frequency of stimulation applied to the LG and MG nerves was initially adjusted to 2 and 3 Hz, respectively. We used TTL-pulses and a Master-8 system to produce simultaneous trains of pulses of stimulation as is illustrated in Fig. 1(A) and (D).

The first stimulation scheme consisted of one sequence that lasted 1 min, during which we applied either a sub-threshold periodic stimulus at 2 Hz to the LG nerve, or a sub-threshold periodic stimulus at 3 Hz to the MG nerve. The second stimulation scheme consisted of one sequence that also lasted 1 min, during which we applied simultaneously trains of sub-threshold stimuli at 2 Hz to the LG nerve, and at 3 Hz to the MG nerve. A third stimulation scheme consisted of 18 sequences that lasted 1 min each in which we examined the case of inharmonic combination of inputs ( $f_1 = 2.1, 2.2, \dots, 2.9$  to LG and  $f_2 = 3.1, 3.2, \dots, 3.9$  to MG). We recorded both the monosynaptic reflexes (MSRs) and the electromyographic (EMGs) activity from the LG and MG muscles elicited by these trains of pulses, and also intracellular potentials in individual motoneurons.

### 2.3. Electrophysiological recordings

We recorded MSRs from the central end of the sectioned L7 ventral root (Fig. 1A) and the gastrocnemius muscles activity. Afferent volleys and cord dorsum potentials (CDPs) (Fig. 1) were recorded at the lumbar segment L7 by means of one silver ball electrode placed on the cord dorsum against an indifferent electrode inserted in the back muscles. We observed that the afferent volleys elicited by stimulation of 2 and 3 Hz to the two nerves (MG and LG) arrived at the cord simultaneously. The size of the MSR was continually monitored during the course of an experiment to assess stability of stimulation and recording conditions (Manjarrez et al., 2005).

EMG recordings of the gastrocnemius muscles (MG and LG) were simultaneously obtained. Low noise and high gain differential amplifiers (Grass model P511) were used to

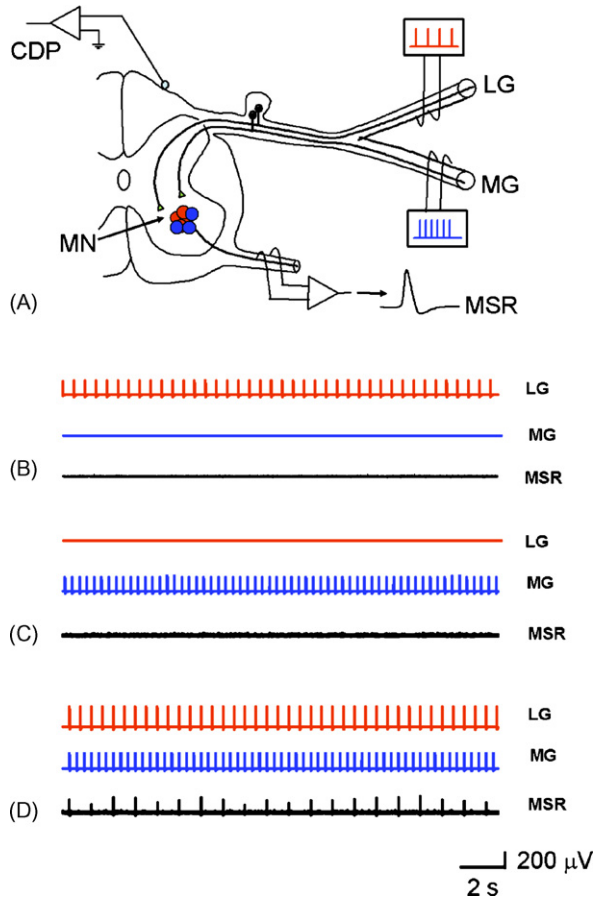


Fig. 1. (A) Scheme of the experimental arrangement. (B) Sub-threshold stimuli at 2 Hz applied to the lateral gastrocnemius (LG) nerve (red). (C) Sub-threshold stimuli at 3 Hz applied to the medial gastrocnemius (MG) nerve (blue). (D) Occurrence of monosynaptic reflexes (MSRs) at the ghost frequency of 1 Hz, a frequency absent in the afferent inputs. Both afferent input signals were 2 and 3 Hz, respectively, and were sub-threshold. In all our experiments we recorded the cord dorsum potentials (CDP) to examine the latency between the afferent volley and the reflex response of the motoneurons (MN). However, for clarity we omitted such recordings in this and in the subsequent illustrations. (For interpretation of the references to colour in this figure legend, the reader is referred to the web version of the article.)

amplify the potentials. For the inharmonic case, time intervals between successive MSRs were measured. We obtained graphs of the instantaneous frequency response versus the frequency of stimulation to the LG nerve.

In other series of experiments intracellular recordings were obtained from motoneurons receiving synaptic inputs from LG and MG afferents. Intracellular recordings were made by means of 3 M potassium acetate-filled micropipettes (tip diameter 1–2  $\mu\text{m}$ ) connected to high-impedance DC amplifier. Motoneurons were identified by their antidromic response to ventral root stimulation. Data acquisition of the intracellular potentials, MSRs, or the gastrocnemius muscle activity was performed with a sampling rate of 10 kHz.

## 2.4. Neural model

We complemented our experimental study by modeling the monosynaptic reflex pathway with a configuration consisting in a pool of 256 motoneurons receiving synaptic stimuli from two input neurons, representing the MG and LG afferent neurons. The dynamical behavior of the membrane potential of each neuron was described by the Morris–Lecar model (Morris and Lecar, 1981):

$$\frac{dV_i}{dt} = \frac{1}{C_m} (I_i^{\text{app}} - I_i^{\text{ion}} - I_i^{\text{syn}}) + D_i \xi(t),$$

$$\frac{dW_i}{dt} = \phi \Lambda(V_i) (W_\infty - W_i), \quad (1)$$

where  $V_i$  and  $W_i$  stand for the membrane potential and the fraction of open potassium channels, respectively. The subindex  $i$  labels the different neurons, with  $i = 1$  and  $2$  representing the two input neurons and the subsequent  $i = 3, \dots, 258$  representing the neurons of the pool.  $C_m$  is the membrane capacitance per unit area,  $I_i^{\text{app}}$  the external applied current and  $I_i^{\text{syn}}$  is the synaptic current. The ionic current is given by

$$I_i^{\text{ion}} = g_{\text{Ca}} M_\infty(V_i) (V_i - V_{\text{Ca}}^0) + g_{\text{K}} W_i (V_i - V_{\text{K}}^0) + g_{\text{L}} (V_i - V_{\text{L}}^0), \quad (2)$$

where  $g_a$  ( $a = \text{Ca}, \text{K}$  and  $\text{L}$ ) is the conductance and  $V_a^0$  is the equilibrium potential of the calcium, potassium and leaking channels, respectively. The following functions of the membrane potential are also defined:

$$M_\infty(V) = \frac{1}{2} \left[ 1 + \tanh \left( \frac{V - V_{M1}}{V_{M2}} \right) \right],$$

$$W_\infty(V) = \frac{1}{2} \left[ 1 + \tanh \left( \frac{V - V_{W1}}{V_{W2}} \right) \right],$$

$$\Lambda(V) = \cosh \left( \frac{V - V_{W1}}{V_{W2}} \right), \quad (3)$$

where  $V_{M1}$ ,  $V_{M2}$ ,  $V_{W1}$  and  $V_{W2}$  are constants specified in Table 1 (Tsumoto et al., in press). The last term in the equation of the membrane potential is a Gaussian white noise term of zero mean and variance  $D_i$ , uncorrelated between neurons, and non-zero only for the neurons of the pool.

The two input neurons are stimulated with trains of square supra-threshold pulses of 1 ms width, amplitudes  $A_{1,2}$  and different frequencies  $f_1$  and  $f_2$ . We used the frequencies  $f_1 = 2 \text{ Hz} + \Delta f$  and  $f_2 = 3 \text{ Hz} + \Delta f$ , with  $\Delta f = 0$  representing the harmonic case. The bias current is  $I_{0,\text{pool}}^{\text{app}} = 42 \mu\text{A}/\text{cm}^2$  for the motoneurons and  $I_{0,1-2}^{\text{app}} = 46 \mu\text{A}/\text{cm}^2$  for the LG and MG neurons, the pulse amplitudes being  $A_{1,2} = 25 \mu\text{A}/\text{cm}^2$  for both frequencies. With this configuration, the two input neurons generate two periodic spike trains, one with frequency  $f_1$  and the other with frequency  $f_2$ , converging on the pool of 256 neurons.

Table 1  
Parameter values of the neuron and synapse models

Parameters	Morris–Lecar TII
$C_m$	5 mF/cm <sup>2</sup>
$g_K$	8 mS/cm <sup>2</sup>
$g_L$	2 mS/cm <sup>2</sup>
$g_{Ca}$	4 mS/cm <sup>2</sup>
$V_K$	−80 mV
$V_L$	−60 mV
$V_{Ca}$	120 mV
$V_{M1}$	−1.2 mV
$V_{M2}$	18 mV
$V_{W1}$	2 mV
$V_{W2}$	17.4 mV
$\phi$	1/15 ms <sup>−1</sup>
Parameters	Synapses
$\alpha$	5 ms <sup>−1</sup>
$\beta$	0.5 ms <sup>−1</sup>
$g_{syn}$	Specified in text
$\tau_{syn}$	1.0 ms
$E_s$	0 mV

### 2.5. Synapse model

For the coupling between the input neurons and the pool neuron, we use a simple model of chemical synapses, which is unidirectional from input neurons to pool neurons. In this model, the synaptic current acting on neuron  $i$  is given by

$$I_i^{syn} = \sum_{j=1,2} g_{ij}^{syn} r_j (V_i - E_s), \quad i = 3, \dots, 258 \quad (5)$$

where the sum runs over the input neurons,  $g_{ij}^{syn}$  is the conductance of the postsynaptic channels,  $r_j$  stands for the fraction of bound receptors of the synaptic channel,  $V_i$  the postsynaptic membrane potential and  $E_s$  is a parameter whose value determines the type of synapses (in this case,  $E_s = 0$  mV and the synapses are excitatory). The fraction of bound receptors,  $r_j$ , follows the equation:

$$\frac{dr_j}{dt} = \alpha [T]_j (1 - r_j) - \beta r_j, \quad (6)$$

where  $[T]_j = \theta(T_j^0 + \tau_{syn} - t)\theta(t - T_j^0)$  ( $\theta$  is the Heaviside step function,  $\theta(x) = 1$  if  $x > 0$  and  $\theta(x) = 0$  if  $x < 0$ ) is a square pulse of width  $\tau_{syn}$  representing the concentration of neurotransmitter released in the synaptic cleft,  $\alpha$  and  $\beta$  are rise and decay time constants, respectively, and  $T_j^0$  is the time at which the presynaptic neuron  $j$  fires, what happens whenever the presynaptic membrane potential exceeds a predetermined value, in our case chosen to be 0 mV. The values of the used parameters are also specified in Table 1.

### 2.6. Numerical setup

The synaptic coupling strength between the input and pool neurons is chosen such that the stimuli are sub-threshold when

they arrive separately, but are supra-threshold when they arrive together, i.e. the neurons of the pool detect the coincidences between the arriving stimuli. This is fulfilled by choosing a synaptic conductance  $g_{pool}^{syn} = 0.5$  mS/cm<sup>2</sup>.

We add some heterogeneity in the synaptic coupling (2%), and also in the excitability threshold (2% in  $I_{0,pool}^{app}$ ) of each neuron of the pool. We also add a small quantity of white noise to the neurons in the pool with amplitude  $D_{pool} = 1.5$  mV/ms.

The equations were integrated using the Heun method (Garcia-Ojalvo and Sancho, 1999), which is equivalent to a second order Runge–Kutta algorithm for stochastic equations.

## 3. Results

### 3.1. First experimental protocol: periodic trains of sub-threshold harmonic stimuli

When two simultaneous sub-threshold stimuli of frequencies 2 and 3 Hz were applied to the LG and MG nerves, respectively, all animals we examined exhibited clear-cut ghost motor responses in their monosynaptic reflexes, as well as in their EMG activity, at 1 Hz frequency. Fig. 1 illustrates the results from one experiment. Fig. 1 (panel B) illustrates a sequence (2 Hz) of sub-threshold stimuli applied to the LG nerve and the absence of MSRs is evident revealing the sub-threshold nature of the signal. Fig. 1 panel C shows the same as Fig. 1B but for the 3 Hz sequence applied to the MG nerve. Fig. 1D shows the occurrence of MSRs at the response frequency of 1 Hz, although both input signals were sub-threshold. Because these responses occurred at a frequency absent in the inputs we defined these reflexes as “ghost motor responses”. In all our experiments we recorded the afferent volleys, but for clarity we omitted such recordings in the illustrations.

The frequency of response at 1 Hz is also well noticeable in the gastrocnemius muscle activation, as can be seen in Fig. 2. This figure shows results obtained from one experiment in which the EMG activity of the LG muscle was recorded. Plots 2B and 2C show that no reflex muscle contractions (EMG muscle responses) were elicited when sub-threshold stimuli were applied to the LG or MG nerves. However, when both sub-threshold stimuli to the LG and MG nerve were simultaneously applied strong LG reflex muscle contractions were observed (Fig. 2D). Similar results were obtained for the MG and LG EMG activity recorded in three other experiments.

The previous observations suggest that ghost excitations occur in both the monosynaptic reflex pathway and gastrocnemius muscles. Fig. 3 shows results from a different experiment in which the intracellular record-

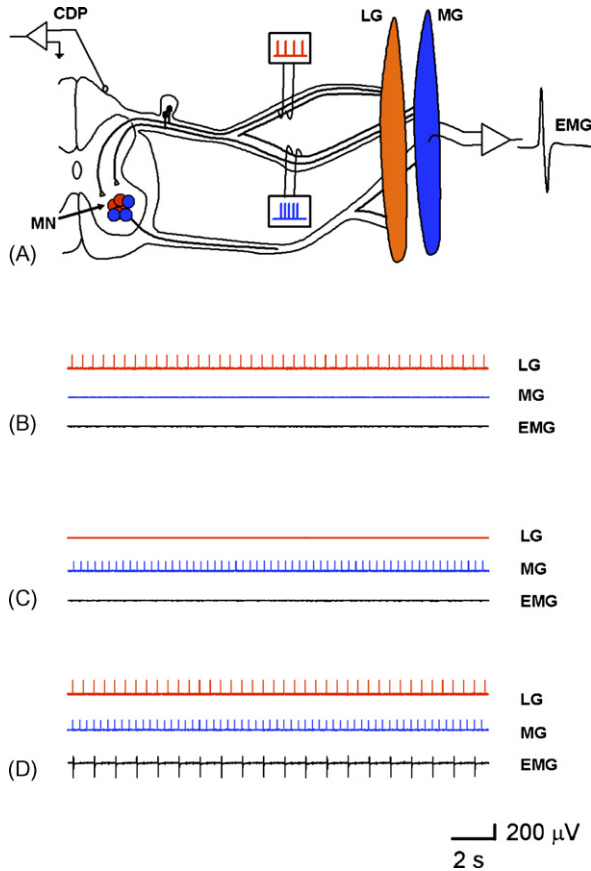


Fig. 2. The same as Fig. 1 but for the electromiographic (EMG) activity. Note that the phantom reflex contractions (i.e., the ghost motor responses) are elicited at a frequency absent in the afferent inputs.

ing of a single motoneuron was obtained. Fig. 3B (3C) illustrates sequences of 2 Hz (3 Hz) of sub-threshold stimuli applied to the LG (MG) nerve. Fig. 3D shows the sequence of action potentials elicited in response to both inputs applied simultaneously, exhibiting a frequency absent in the inputs. Similar results were obtained in two other motoneurons.

### 3.2. Second experimental protocol: trains of sub-threshold inharmonic stimuli

To further investigate in detail the ghost motor responses we considered an inharmonic situation in which stimuli to LG and MG nerves were sub-threshold. In sub-threshold conditions the stimuli were able to produce a muscle contraction only when a perfect coincidence among the postsynaptic responses occurred.

We simultaneously applied sub-threshold pulses of frequency  $2 \text{ Hz} + \Delta f$  to LG nerve and  $3 \text{ Hz} + \Delta f$  to MG

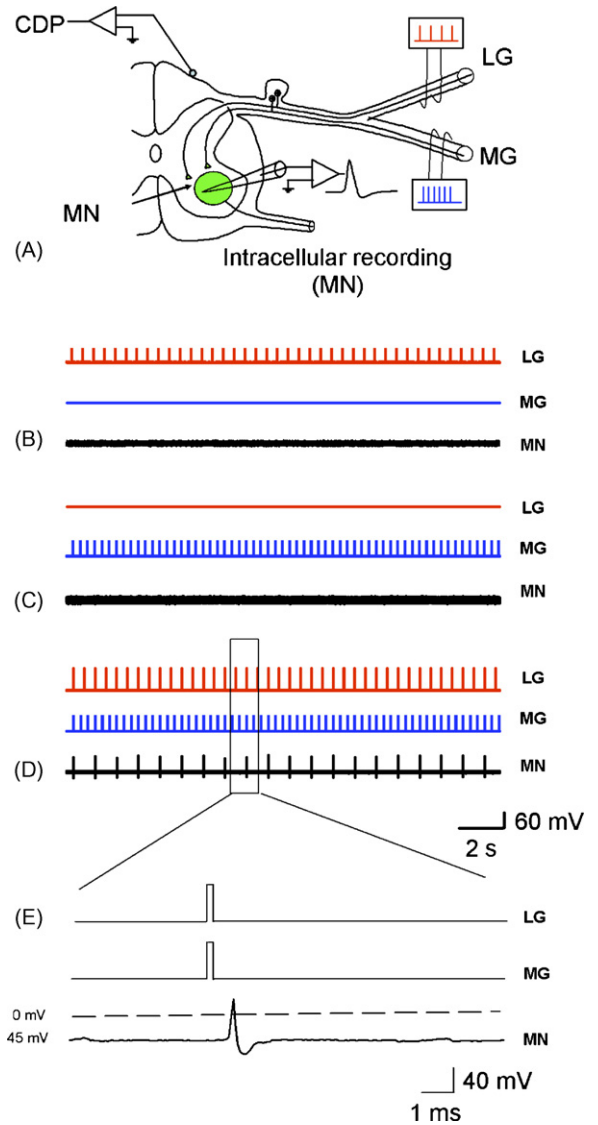


Fig. 3. (A–D) The same as Fig. 1(A)–(D) but for the intracellular recording of one motoneuron. This result is consistent with Figs. 1 and 2.

nerve.  $\Delta f$  is the frequency shift, equal to both inputs, and was varied by 0.1 Hz steps from 0.1 to 1.9 Hz. Our experimental results revealed that the ghost motor frequency is much lower than both  $f_1$  and  $f_2$ . In Fig. 4A we plot a typical time trace of the MSR recorded at the L7 ventral root for a given  $\Delta f$  (in this case  $\Delta f = 0.3 \text{ Hz}$ ). Note that the ghost motor responses (inferred from the MSR) occurred every 10 seconds. A simple inspection of this figure allowed us to corroborate that the ghost frequency (0.1 Hz in this case) corresponds to that at which a perfect coincidence between the spikes generated by the two input excitations on the pool occurred.



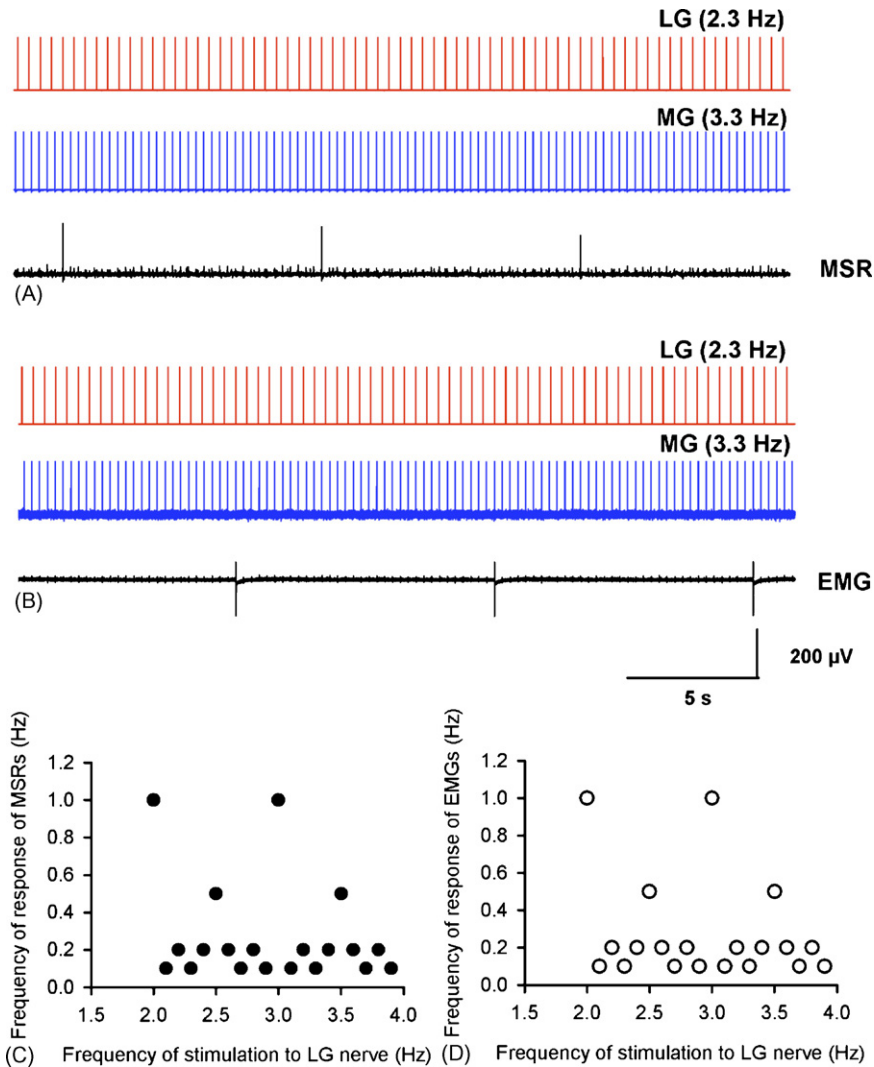


Fig. 4. Monosynaptic reflexes (MSRs) (A) and electromyographic (EMG) (B) recordings, illustrating the ghost motor responses at a frequency of 0.1 Hz. Both input signals of 2.3 and 3.3 Hz, were sub-threshold. (C–D) Frequency of stimulation to the LG nerve vs. the frequency of response of the MSRs (C) and EMGs (D).

Consequently, the nervous system is acting as a detector for coincidences of low-frequency ghost signals and explains the observed response of the MSRs (Lopera et al., 2006). These conclusions were further checked by recording the gastrocnemius muscle activity. In Fig. 4B we show a time trace of the recorded muscle activity (EMG) for  $\Delta f=0.3$  Hz, as in Fig. 4A. Again the presence of a low frequency ghost motor response is evident. Plots 4C and 4D show the frequency response of the MSRs and EMGs, respectively, as a function of the frequency shift; in those plots the slow activation is evident. Similar results to those illustrated in Fig. 4 were obtained from intracellular recordings of three motoneurons.

### 3.3. Numerical results

We numerically solved the model described above, using the parameters given in Table 1. We considered different pairs of input frequencies  $f_1$  and  $f_2$ , ranging from  $f_1 = 2$  Hz and  $f_2 = 3$  Hz up to  $f_1 = 3.9$  Hz and  $f_2 = 4.9$  Hz, increasing the frequency in steps of  $\Delta f=0.1$  Hz. For each pair of frequencies, we made simulations over a time span of 60 s, with a time step of 0.01 ms.

In Fig. 5 we plot two temporal numerical series of the membrane potential, averaged over the motoneuron pool, corresponding to the harmonic case  $f_1 = 2$  Hz and  $f_2 = 3$  Hz (panel B) and an inharmonic case  $f_1 = 2.1$  Hz and  $f_2 = 3.1$  Hz (panel C). Panel B clearly shows that

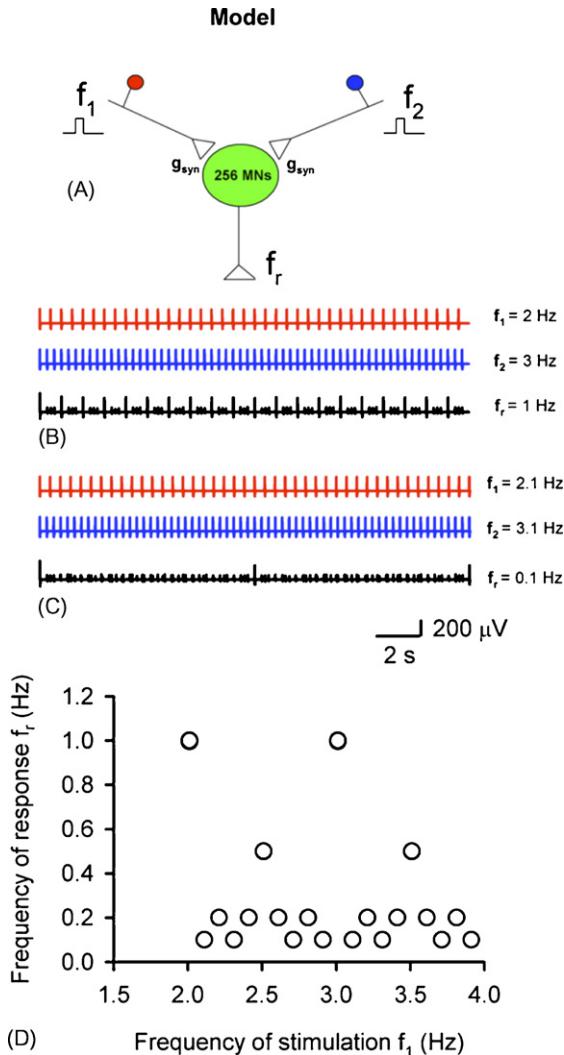


Fig. 5. (A) Scheme of the theoretical model, consisting of a pool of 256 motoneurons to which two input pulse trains are applied. Average membrane potential of the pool of motoneurons as obtained from numerical simulations, when the input frequencies are: (B) 2.0 and 3.0 Hz (harmonic case) and (C) 2.1 and 3.1 Hz (a particular instance of an inharmonic case). Perfect coincidences occur with frequency 1 Hz in case (B) and 0.1 Hz in case (C). (D) Ghost response frequency (inverse of the inter-spike time interval) as a function of one of the input frequencies ( $f_1$ ) obtained from numerical simulations.

the motoneuron pool responds at the ghost frequency 1 Hz in the harmonic case. In Fig. 5D, we plot the instantaneous response frequency  $f_r$  (the inverse of inter-spike time in the average membrane potential) versus one of the input frequencies,  $f_1$ , when the latter varies from 2.0 to 3.9 Hz in steps of  $\Delta f = 0.1$  Hz. The results shown in this figure are in very good agreement with the experiments. The distribution of points can be easily understood if we take into account that the phenomena

relies in a coincidence detection mechanism of very narrow pulses. In the harmonic case of two spike trains of frequencies 2 and 3 Hz, whose periods are 1/2 and 1/3 s, coincidences will arise (if the relative phase of the signals is properly chosen) every 1 s, i.e., with a frequency of 1 Hz. On the other hand, in an inharmonic case such as that where the input frequencies are 2.1 and 3.1 Hz, the signals will coincide exactly every 10 s, i.e. with frequency of 0.1 Hz. This response frequency becomes 0.2 Hz (corresponding to perfect coincidences every 5 s) when the input frequencies are 2.2 and 3.2 Hz, but decays again to 0.1 Hz when the input frequencies are 2.3 and 3.3 Hz. This simple calculation can be extended for all values of the input frequencies shown in Fig. 5D. The model confirms the existence of ghost motor responses when two synaptic afferent inputs are involved.

#### 4. Discussion

##### 4.1. An explanation for the origin of the ghost motor responses

Stimuli applied to LG and MG Ia afferents produce monosynaptic reflex responses, which can be recorded in motoneurons, ventral roots or in muscles. How can the muscles respond with contractions at a frequency physically absent in the sub-threshold input stimuli? We presented experimental and numerical evidence of ghost motor responses of the cat spinal cord. When applying simultaneously distinct sub-threshold signals to the LG and MG nerves we observed repetitive motor responses at a low-frequency not present in the input. In the harmonic case, the MSR, action potentials of motoneurons, and muscle responses appeared at a frequency equal to the difference between the frequencies of the input signals. In the inharmonic case the resonance was observed at much lower frequencies (0.1–0.5 Hz), at which an exact coincidence between the two spike responses to the input signals occurred, highlighting the coincident detection effect and the concomitant summation of the postsynaptic potentials from the two convergent inputs (LG and MG). Furthermore, the ghost motor responses exhibited by single motoneurons clearly occurred (monosynaptically) after the exact coincidence between the inputs, as was illustrated in Fig. 3E. A simple inspection of Fig. 3E allowed us to corroborate that the ghost motor frequency of 1 Hz (in this case) corresponds to that at which a perfect coincidence between the two input excitations on the pool occurred. Similar results were obtained for the inharmonic case, for example for the 2.3 and 3.3 Hz frequency inputs, illustrated in Fig. 4A and B,

where the motor responses occurred at a low frequency determined by the perfect coincidence between the two input excitations (0.1 Hz in that case). Consequently, the monosynaptic reflex pathway of the cat is acting as a detector for exact coincidences of low-frequency ghost signals and explains the observed ghost motor responses of the MSRs, EMGs, and action potentials in single motoneurons.

#### 4.2. Determinants of coincidence detection

The coincidence detection mechanism also merits a discussion in this paper. A coincidence detection of convergent synaptic inputs on one neuron refers to their capacity to produce an action potential when the inputs act simultaneously. Several studies use the probability of occurrence of such action potentials as a measure of the effectiveness of coincidence detection (Kuba et al., 2002). Some forms of synaptic plasticity depend on the temporal coincidence of presynaptic activity and postsynaptic response (Montague and Sejnowski, 1994). The synaptic response associated with the coincidence detection depends on the duration of the convergent excitatory postsynaptic potentials (EPSPs) by determining the time window within which they summate to produce an action potential (Cathala et al., 2003). There are some evidences suggesting that thin EPSPs allow neurons to behave as good coincidence detectors, whereas wide EPSPs provide a mechanism by which the neurons could behave as temporal integrators (Trussell, 1997; Taschenberg and von Gersdorff, 2000; Kuba et al., 2002; Cathala et al., 2003). Our results are consistent with the first case. In this context, the exact coincidence detection of the afferent inputs from the LG and the MG nerves may provide great accuracy to their motor responses. Further studies would be necessary to examine if the synaptic background activity impinging on motoneurons could act as a switch between the temporal integration and the coincidence detection, as in pyramidal neurons (Rudolph and Destexhe, 2003).

The mechanism of coincidence detection has been extensively studied in the detection of the inter-aural time difference of the sound in the auditory system. For example, the neurons from the nucleus laminaris of the chicken generate action potentials at maximal probability when bilateral inputs arrive in coincidence (Kuba et al., 2002). Furthermore, there are some evidences that the degree of accuracy in the coincidence detection of the auditory neurons can be modulated by changes in temperature, extracellular sodium concentration, dendrotoxine concentration, or during development (Kuba et al., 2002; Svirakis et al., 2003, 2004). In this

context, further work will be necessary to determine if a similar modulation of the degree of accuracy in the coincidence detection could also occur in the monosynaptic reflex pathway, thus affecting their ghost motor responses.

#### 4.3. Difference in the ghost responses between the auditory and the motor system

We suggest that the difference in the ghost responses between the auditory and the motor systems could be explained by the dynamical range of detection of these systems. The standard ghost stochastic resonance (GSR) modeled by Balenzuela and Garcia-Ojalvo (2005) is reproduced when the window of detection is about 30 ms, but is absent when it is restricted to about 2 ms (results to be published in a subsequent study). In this context, we suggest that in the auditory pathway the window of detection is wider compared to that of the monosynaptic reflex pathway of the cat spinal cord. This suggestion is in agreement with experimental evidence that EPSPs evoked in some cochlear nuclei neurons (e.g. fusiform and stellate) have durations of about 10 to 100 ms (Ferragamo et al., 1998; Zhang and Oertel, 1994), in contrast to the short duration of about 5 ms of the EPSPs evoked by the motoneurons. These physiological facts could explain the discrepancies between the ghost responses associated to the GSR in the auditory system, and those that we have observed for the motor pathway.

#### 4.4. Robustness against noise and phase shift

As shown in the paper, the appearance of phantom reflexes relies on a coincidence detection mechanism. This mechanism is indeed compromised by phase shift among the periodic inputs. In previous work (Balenzuela and Garcia-Ojalvo, 2005) the robustness of the coincidence detection mechanism was tested, and we expect the same behavior here. In the mentioned work, the train pulse generated by the input neurons was randomly distributed around the period of the stimulus, due to noise. It was seen that the wider the distribution of inter-spike intervals, the less efficient the neuron was to detect coincidences. Nevertheless, the global response of the system was, on average, at the expected missing frequency.

Therefore, in the present case we also expect that, if the inter-spike intervals generated by the input neurons were distributed around the input frequencies, instead of exhibiting single peaked distributions, the motoneurons would respond at the same phantom frequency, even if less efficiently.



#### 4.5. Physiological significance and implications

The central nervous system continuously integrates the input from synergistic Ia afferents with two aims: (1) to produce movements of a limb via the motoneurons and (2) to perceive real or illusory limb movements.

Regarding the first aim, we would like to speculate that in normal physiological conditions in humans the ghost motor responses participate in the integration of synergistic Ia-afferent input. This possibility is based on the fact that the triceps surae muscles are a synergistic unit composed of three muscles, i.e., LG, MG and soleus muscles. In normal conditions these muscles are activated in synergy in many movements. Both LG and MG muscles will be activated in synergy only when the convergent inputs from Ia afferents are simultaneously acting on LG and MG motoneurons. For example, as a security factor, a possible LG undesired stretching (at a different frequency) should not be enough to produce a reflex contraction of the MG muscle, thus avoiding the undesired contraction of the whole triceps surae muscle, or the undesired consequent movement of the whole hindlimb. Such a response will only occur at the frequency of coincidence in the MG and LG Ia-afferent volleys. In these conditions, stimuli of different frequencies acting upon the LG and MG motoneurons would elicit a ghost motor response as described above.

Regarding the second aim, we would like to speculate that in physiological conditions in humans the ghost motor responses participate in the perception of illusory limb movement. There are evidences that perception of limb movements does not necessarily require the actual movement of the limbs (Collins et al., 2005). Vibration stimuli of about 70 Hz exciting a group of synergistic muscle spindles induce illusory movement of low frequency. Verschueren et al. (1998) demonstrated that the central nervous system uses Ia-afferent input from synergistic muscles at a joint to construct a perception of the kinematics of movement. Furthermore, Naito et al. (1999) reported that in humans these illusory arm movements elicited by vibration are associated with the activation of cortical motor areas. Therefore, because the input frequencies of the vibratory stimuli applied to synergistic muscles are about 70 Hz (high frequency) and the resultant illusory movement is perceived at a low frequency, then we suggest that a kind of ghost motor response at the cortical stage is occurring. This could be possible because the illusory movement was perceived at a frequency physically absent in the input (70 Hz).

From a physiological perspective we suggest that the ghost motor responses in both cases of illusory and real movement are elicited in part by the synergism among

different Ia-afferent inputs. This possibility is substantiated by the fact that the brain requires input from more than one muscle Ia spindle afferent to perceive movement (Macefield et al., 1990). These authors observed that stimulation of a single muscle spindle afferent did not evoke a perception of movement. However, there is evidence that simultaneous vibration of two muscles in the stationary wrist of human subjects results in a single illusion with a specific direction (Roll and Gilhodes, 1995).

It is also possible that in humans the ghost motor responses could participate in the integration of synergistic Ia-afferent input during the fatiguing muscle contractions at a low frequency absent in the inputs. This could be possible because during a voluntary prolonged contraction there is a sustained high frequency firing from synergistic Ia afferents via the alpha-gamma coactivation (Vallbo, 1981). This possibility of a ghost motor response during the fatigue is based in a study performed by Tamaki et al. (1998) in normal humans. These authors reported that during prolonged low-level fatiguing contractions of the triceps surae muscle there is an alternate activity of the synergistic muscles (MG and LG) occurring at a low frequency. They observed that EMG recordings showed alternation between activation and inactivation in individual muscles during prolonged static contractions. It is not easy to explain how this alternate activity occurs. A possibility is that during the fatiguing process convergent afferent inputs of high frequencies from LG and MG Ia afferents produce episodes of absence of coincidence between both convergent inputs on the motoneurons. Such an absence of coincidence could be the cause of the silent periods of the muscle activity observed in the fatiguing stage. Because the episodes of activity and silence occurred at a low frequency absent in the input frequency from the Ia afferents to the motoneurons we speculate that this motor response of low frequency also could be a kind of ghost motor response.

We conclude that the simple coincidences of sub-threshold convergent synaptic inputs on one motoneuron can evoke action potentials and subsequent contractions of the innervated muscle cells at a frequency physically absent in their inputs, i.e., a ghost motor response. Therefore, motoneurons are robust detectors of coincidences of monosynaptic inputs from Ia afferents, which respond to the summation of postsynaptic potentials. We suggest that the explanation of the ghost motor responses of the spinal cord could be useful to further understand similar phenomena in more complex systems, as in the auditory system, in which the physiological mechanisms by which the nervous system integrates sensory information

at a frequency physically absent in the binaural sensory inputs have not been directly revealed yet.

## Acknowledgements

We thank D.R. Chialvo for helpful comments. This work was partly supported by the following grants: CONACyT J36062-N (E.M), Fondo-Ricardo J. Zevada (A.F) and FOMES-BUAP, México; MEC (Spain) and Feder projects BFM2003-07850 and FIS2004-00953, and Generalitat de Catalunya. We thank Alma G. López for technical assistance. Pablo Balenzuela is member of Carrera de Investigador de Conicet, Departamento de Física, Universidad de Buenos Aires, Argentina.

## References

- Balenzuela, P., Garcia-Ojalvo, J., 2005. Neural mechanism for binaural pitch perception via ghost stochastic resonance. *Chaos* 15, 023903.
- Cathala, L., Brickley, S., Cull-Candy, S., Farrant, M., 2003. Maturation of EPSCs and intrinsic membrane properties enhances precision at a cerebellar synapse. *J. Neurosci.* 23, 6074–6085.
- Chialvo, D.R., 2003. How we hear what is not there: a neural mechanism for the missing fundamental illusion. *Chaos* 13, 1226–1230.
- Collins, D.F., Refshauge, K.M., Todd, G., Gandevia, S.C., 2005. Cutaneous receptors contribute to kinesthesia at the index finger, elbow, and knee. *J. Neurophysiol.* 94, 1699–1706.
- Ferragamo, M.J., Golding, N.L., Oertel, D., 1998. Synaptic inputs to stellate cells in the ventral cochlear nucleus. *J. Neurophysiol.* 79, 51–63.
- Garcia-Ojalvo, J., Sancho, J.M., 1999. *Noise in Spatially Extended Systems*. Springer-Verlag, New York.
- Granit, R., Kernell, D., Lamarre, Y., 1966. Algebraic summation in synaptic activation of motoneurons firing within the primary range to injected currents. *J. Physiol. (Lond.)* 187, 379–399.
- Kuba, H., Koyano, K., Ohmori, H., 2002. Development of membrane conductance improves coincidence detection in the nucleus laminaris of the chicken. *J. Physiol.* 540, 529–542.
- Kuno, M., Miyahara, J.T., 1969. Non-linear summation of unit synaptic potentials in spinal motoneurons of the cat. *J. Physiol. (Lond.)* 201, 465–477.
- Lloyd, D.P.C., 1946. Facilitation and inhibition of spinal motoneurons. *J. Neurophysiol.* 9, 421–438.
- Lopera, A., Buldú, J.M., Torrent, M.C., Chialvo, D.R., García-Ojalvo, J., 2006. Ghost stochastic resonance with distributed inputs in pulse-coupled electronic neurons. *Phys. Rev. E* 73, 021101-1–6.
- Macefield, G., Gandevia, S.C., Burke, D., 1990. Perceptual responses to microstimulation of single afferents innervating joints, muscles and skin of the human hand. *J. Physiol. (Lond.)* 429, 113–129.
- Manjarrez, E., Rojas-Piloni, G., Méndez, Flores, A., 2003. Stochastic resonance within the somatosensory system: effects of noise on evoked field potentials elicited by tactile stimuli. *J. Neurosci.* 23, 1997–2001.
- Manjarrez, E., Hernández-Paxtián, Z., Kohn, A., 2005. Spinal source for the synchronous fluctuations of bilateral monosynaptic reflexes in cats. *J. Neurophysiol.* 94, 3199–3210.
- Montague, P.R., Sejnowski, T.J., 1994. The predictive brain: temporal coincidence and order in synaptic learning mechanisms. *Learn. Mem.* 1, 1–33.
- Morris, C., Lecar, H., 1981. Voltage oscillations in the barnacle giant muscle fiber. *Biophys. J.* 35, 193–213.
- Naito, E., Ehrsson, H.H., Geyer, S., Zilles, K., Roland, P.E., 1999. Illusory arm movements activate cortical motor areas: a positron emission tomography study. *J. Neurosci.* 19 (14), 6134–6144.
- Rudolph, M., Destexhe, A., 2003. Tuning neocortical pyramidal neurons between integrators and coincidence detectors. *J. Comput. Neurosci.* 14, 239–251.
- Roll, J.P., Gilhodes, J.C., 1995. Proprioceptive sensory codes mediating movement trajectory perception: human hand vibration-induced drawing illusions. *Can. J. Physiol. Pharmacol.* 73 (2), 295–304.
- Svirakis, G., Dodla, R., Rinzel, J., 2003. Subthreshold outward currents enhance temporal integration in auditory neurons. *Biol. Cybern.* 89, 333–340.
- Svirakis, G., Kotak, V., Sanes, D., Rinzel, J., 2004. Sodium along with low-threshold potassium currents enhance coincidence detection of subthreshold noisy signals in MSO neurons. *J. Neurophys.* 91, 2465–2473.
- Tamaki, H., Kitada, K., Akamine, T., Murata, F., Sakou, T., Kurata, H., 1998. Alternate activity in the synergistic muscles during prolonged low-level contractions. *J. Appl. Physiol.* 84 (6), 1943–1951.
- Taschenberg, H., von Gersdorff, H., 2000. Fine-tuning an auditory synapse for speed and fidelity: developmental changes in presynaptic waveform, EPSC kinetics, and synaptic plasticity. *J. Neurosci.* 20, 9162–9173.
- Trussell, L.O., 1997. Cellular mechanisms for preservation of timing in central auditory pathways. *Curr. Opin. Neurobiol.* 7, 487–492.
- Tsumoto, K., Kitajima, H., Yoshinaga, Y., Aihara, K., Kawakami, H., in press. Bifurcations in Morris–Lecar neuron model. *Neurocomputing*.
- Verschueren, S.M., Cordo, P.J., Swinnen, S.P., 1998. Representation of wrist joint kinematics by the ensemble of muscle spindles from synergistic muscles. *J. Neurophysiol.* 79 (5), 2265–2276.
- Vallbo, A.B., 1981. Basic patterns of muscle spindle discharge in man. In: Taylor, A., Prochazka (Eds.), *Muscle Receptors and Movement*. Macmillan, London, pp. 263–275.
- Zhang, S., Oertel, D., 1994. Neuronal circuits associated with the output of the dorsal cochlear nucleus through fusiform cells. *J. Neurophysiol.* 71, 914–930.